

Model for the regulation of *Arabidopsis thaliana* leaf margin development

Gemma D. Bilborough^{a,1}, Adam Runions^{b,1}, Michalis Barkoulas^{a,1,2}, Huw W. Jenkins^a, Alice Hasson^c, Carla Galinha^a, Patrick Laufs^c, Angela Hay^a, Przemyslaw Prusinkiewicz^{b,3}, and Miltos Tsiantis^{a,3}

^aDepartment of Plant Sciences, University of Oxford, Oxford OX1 3RB, United Kingdom; ^bDepartment of Computer Science, University of Calgary, Calgary, AB, Canada T2N 1N4; and ^cLaboratoire de Biologie Cellulaire, Institut Jean Pierre Bourgin, Institut National de la Recherche Agronomique, 78026 Versailles Cedex, France

Edited* by Mark Estelle, University of California at San Diego, La Jolla, CA, and approved January 7, 2011 (received for review October 17, 2010)

Biological shapes are often produced by the iterative generation of repeated units. The mechanistic basis of such iteration is an area of intense investigation. Leaf development in the model plant *Arabidopsis* is one such example where the repeated generation of leaf margin protrusions, termed serrations, is a key feature of final shape. However, the regulatory logic underlying this process is unclear. Here, we use a combination of developmental genetics and computational modeling to show that serration development is the morphological read-out of a spatially distributed regulatory mechanism, which creates interspersed activity peaks of the growth-promoting hormone auxin and the CUP-SHAPED COTYLEDON2 (*CUC2*) transcription factor. This mechanism operates at the growing leaf margin via a regulatory module consisting of two feedback loops working in concert. The first loop relates the transport of auxin to its own distribution, via polar membrane localization of the PIN-FORMED1 (*PIN1*) efflux transporter. This loop captures the potential of auxin to generate self-organizing patterns in diverse developmental contexts. In the second loop, *CUC2* promotes the generation of *PIN1*-dependent auxin activity maxima while auxin represses *CUC2* expression. This *CUC2*-dependent loop regulates activity of the conserved auxin efflux module in leaf margins to generate stable serration patterns. Conceptualizing leaf margin development via this mechanism also helps to explain how other developmental regulators influence leaf shape.

Leaf margin morphology is commonly used to distinguish different plant species and often evolves in close correspondence with the environment. For example, the degree of leaf serration is a good predictor of mean annual temperature of landmasses over geological timescales (1). Variations in margin morphology were first documented in antiquity (2) and were among the first heritable traits studied in plants (3). Nonetheless, a predictive model of leaf margin shape acquisition is lacking. Recent genetic analyses have revealed two key processes required for serration formation: regulated auxin transport by the efflux carrier PINFORMED1 (*PIN1*) (4) and activity of the growth repressor CUP-SHAPED COTYLEDON2 (*CUC2*), which is negatively regulated by miR164 (5). *PIN1* has a polar subcellular localization and forms convergence points at the margins of leaves, creating localized auxin activity maxima that are required for the outgrowth of serrations (4, 6). Leaves of both *pin1* and *cuc2* mutants fail to initiate serrations and have smooth margins, highlighting the importance of these gene products for leaf morphogenesis (4, 5). Here, we show how *CUC2* activity and auxin transport and signaling are regulated and integrated to sculpt leaf margin serrations.

Results

Interspersed *CUC2* and Auxin Activity Maxima Underpin Serration Formation. To understand the dynamics of *CUC2* and auxin activity during serration development, we monitored *CUC2::CUC2:VENUS* expression and the auxin response sensor *DR5::GFP*. Before serration outgrowth, *DR5::GFP* is restricted to the leaf tip and absent from the leaf margin, whereas *CUC2::CUC2:VENUS* is expressed

along the margin (Fig. 1*A*). A focus of *DR5::GFP* expression then emerges at a site of serration initiation, which correlates with repression of *CUC2::CUC2:VENUS* (Fig. 1*B*). As the leaf margin grows, subsequent auxin activity foci appear in a basipetal sequence at positions where *CUC2::CUC2:VENUS* expression is lost and further serrations form (Fig. 1*C*). We, therefore, hypothesized that this interspersed distribution of auxin activity maxima and *CUC2* expression at the leaf margin underpins serration development. We tested this hypothesis by abolishing this interspersed pattern and examining the impact on serration formation. First, we created a continuous marginal domain of *CUC2* expression using an *AtMLI::CUC2:VENUS* transgene to express *CUC2* throughout the epidermis (Fig. 1*D–G* and Fig. S1*A–D*) (7). Second, we applied auxin exogenously to create a continuous distribution of auxin (Fig. 1*H* and *I*). Both treatments yielded leaves with smooth margins, suggesting that continuous *CUC2* or auxin activity is sufficient to prevent serration formation. Epidermal expression of *CUC2* caused additional defects, including leaves with fewer or aberrantly positioned serrations and cup-shaped cotyledons similar to those observed in *cuc1*; *cuc2* double mutants (Fig. 1*J* and *K*). These defects further highlight the significance of discontinuities in *CUC2* expression for proper *CUC* function during development.

***CUC2* and Auxin Activity Maxima Are Regulated in a Feedback Loop via *PIN1*.** To investigate the regulatory relationship between *CUC2* and *PIN1* during serration development, we analyzed auxin activity and *PIN1* localization in *cuc2* leaf margins. In contrast to wild type, *DR5::GFP* expression foci are absent along the margin during early leaf development in *cuc2* mutants and are present only at the leaf tip (Fig. 2*A* and *B*, 500- μ m leaf length). This expression becomes diffuse around the margins of *cuc2* leaves later in development (Fig. 2*C–F*, 750- μ m leaf length, see ref. 8) and resembles the expression of *DR5* in response to auxin transport inhibition (4). This pattern of auxin activity is associated with a lack of *PIN1* convergence points in the *cuc2* margin (Fig. 2*G* and *H* and Fig. S1*E* and *F*). However, *PIN1* localization remains polar in each cell. Therefore, *CUC2* is re-

Author contributions: G.D.B., A.R., M.B., P.L., A. Hay, P.P., and M.T. designed research; G.D.B., A.R., M.B., A. Hasson, A. Hay, and P.P. performed research; H.W.J. contributed new reagents/analytic tools; G.D.B., A.R., M.B., P.L., A. Hay, P.P., and M.T. analyzed data; and G.D.B., A.R., C.G., A. Hay, P.P., and M.T. wrote the paper.

The authors declare no conflict of interest.

*This Direct Submission article had a prearranged editor.

Freely available online through the PNAS open access option.

¹G.D.B., A.R., and M.B. contributed equally to this work.

²Present address: Institut Jacques Monod, Centre National de la Recherche Scientifique–University Denis Diderot–Paris 7–Université Pierre et Marie Curie, 75251 Paris Cedex 05, France.

³To whom correspondence may be addressed. E-mail: miltos.tsiantis@plants.ox.ac.uk or pwp@cps.ucalgary.ca.

This article contains supporting information online at www.pnas.org/lookup/suppl/doi:10.1073/pnas.1015162108/-DCSupplemental.

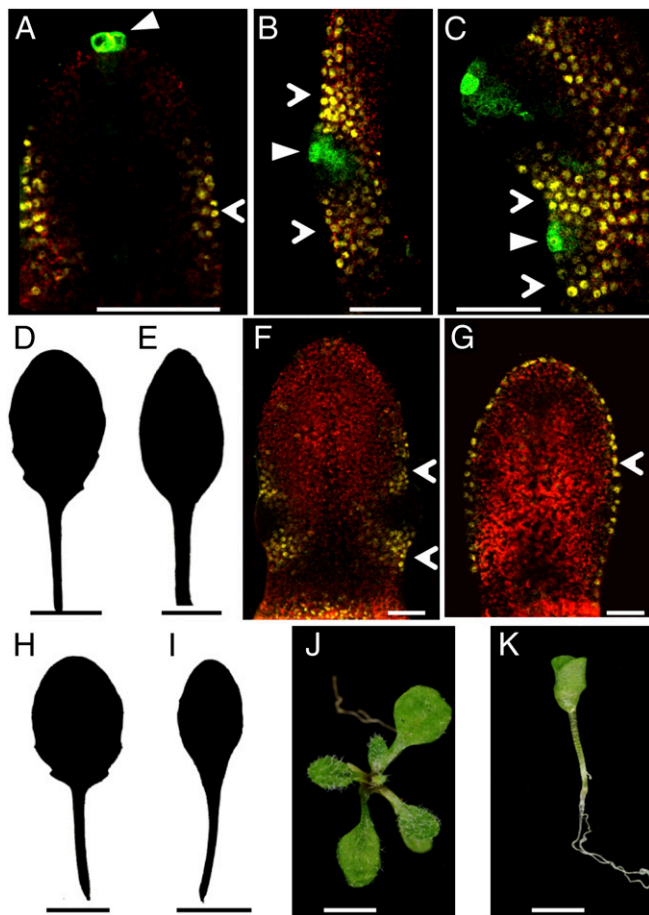


Fig. 1. Interspersed *CUC2* expression and auxin activity maxima are required for serration development. (A–C) Confocal micrographs showing *CUC2::CUC2::VENUS* (yellow, open arrowhead) and *DR5::GFP* (green, closed arrowhead) expression in fifth rosette leaf 130 μm in length (A), serration of fifth rosette leaf 365 μm in length (B), and serrations of fifth rosette leaf 460 μm in length (C). (D and E) Silhouette of fifth rosette leaf of control (D) and *AtML1::CUC2::VENUS* with smooth leaf margin (E). (F and G) Confocal micrograph of single optical section of fifth rosette leaf 370 μm in length of *CUC2::CUC2::VENUS* (F; yellow, open arrowhead) and *AtML1::CUC2::VENUS* (G; yellow, open arrowhead) expression. (H and I) Silhouette of fifth rosette leaf of mock-treated (H) and 10 μM 2,4-D-treated (I) wild-type plants. (J and K) Whole seedlings of hygromycin-resistant control (J) and *AtML1::CUC2::VENUS* with cup-shaped cotyledons (K). (Scale bars: A–C, F, and G, 25 μm ; D, E, and H–K, 1 cm.)

quired to generate PIN1 convergence points that are necessary for localized auxin activity and serration outgrowth.

In addition, we observed an inhibitory relationship between auxin and *CUC2* transcription, as auxin repressed the expression of a *CUC2::GUS* transcriptional reporter gene (Fig. 2 I–L and Fig. S1 G and H). This repression was seen in response to auxin treatment and in *pin1* mutants, in which auxin likely accumulates at the leaf margin (4, 6). Our data showed that auxin can also repress *CUC2* posttranscriptionally via *MIR164A* activation. We found that elevated *CUC2* levels as a consequence of reduced *MIR164A* expression were responsible for the pronounced serrations in two auxin signaling mutants, *auxin resistant1* (*axr1*) and *bodenlos* (*bdl/BDL*) (Fig. 3 A–I, Fig. S1 I–O, and Table S1). Such genetic analyses also suggested a strict requirement for both *CUC2* and PIN1 in serration development: We found that elevated *CUC2* levels cannot trigger serrations in the absence of PIN1 activity (double mutants between *pin1* and either *mir164a* or *mir164*-resistant *CUC2* lack serrations, Fig. S1 P–V) and,

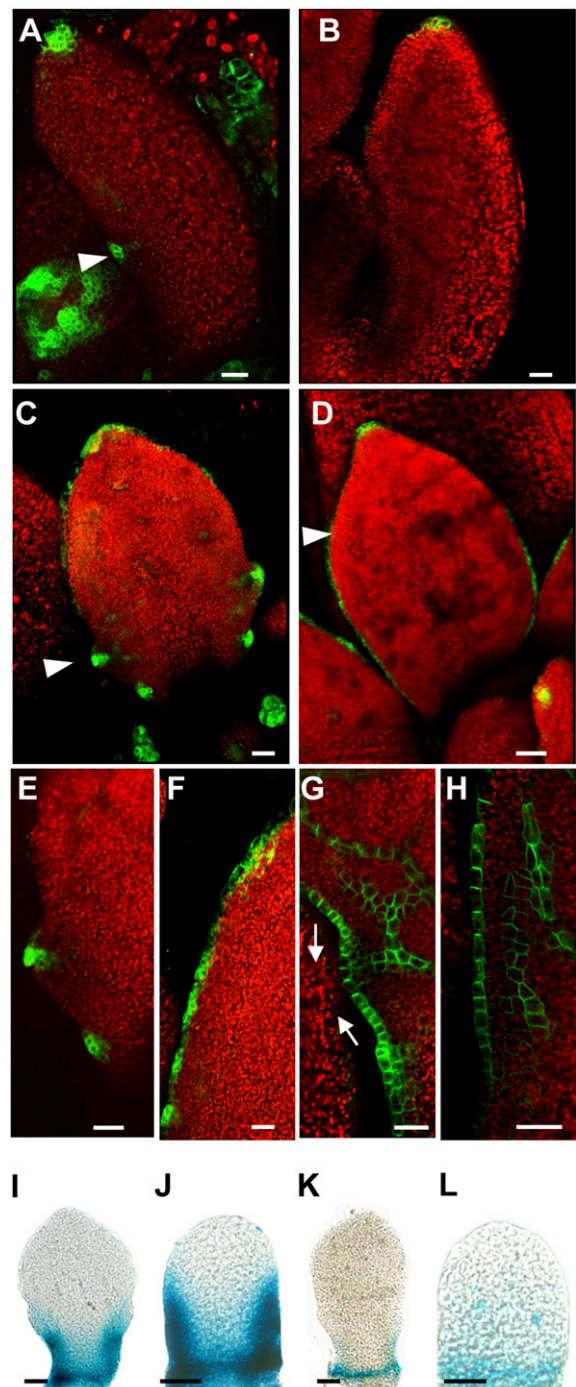


Fig. 2. Feedback regulation between *CUC2* and auxin activity maxima via PIN1. (A–F) Confocal micrographs of *DR5::GFP* expression (green, arrowhead) in sixth rosette leaf 500 μm in length (A and B), fifth rosette leaf 750 μm in length (C and D), and close-up of fifth rosette leaf 750 μm in length (E and F) in wild type (A, C, and E) and *cuc2-3* (B, D, and F). (G and H) Confocal micrographs of *PIN1::PIN1::GFP* expression (green) in close-up of fifth rosette leaf 750 μm in length in wild type (G) and *cuc2-3* (H). Arrows indicate auxin convergence point. (I–L) *CUC2::GUS* staining in sixth rosette leaf 350 μm in length (I and K) and eighth rosette leaf 190 μm in length (J and L) following mock treatment (I and J) or 1 μM IAA treatment (K and L). (Scale bars: A–H, 25 μm ; I–L, 50 μm .)

equally, impaired auxin signaling cannot trigger serrations in the absence of *CUC2* (*axr1;cuc2* and *bdl/BDL;cuc2* double mutants lack serrations, Fig. 3 A–F). Taken together, these data reveal

the operation of a feedback loop that is critical for serration development. Within this loop, *CUC2* promotes the establishment of PIN1 convergence points that generate auxin maxima, which in turn repress *CUC2* expression. These interactions generate a pattern of auxin maxima interspersed with *CUC2* expression along the leaf margin.

Epidermal PIN1 Activity Is Sufficient to Regulate Morphogenetic Events in the Leaf. To test whether PIN1 activity in the epidermis alone is sufficient for serration development, we expressed *AtML1::PIN1::GFP* in *pin1* mutants. We observed that epidermal expression of *AtML1::PIN1::GFP* can restore serration formation in these leaves (Fig. 4 *A–G* and Fig. S2 *A–E*). PIN1 convergence points in the leaf epidermis not only are required for serration patterning, but also mark sites where auxin is transported to internal tissue layers and guides the development of vasculature (4, 6). We found that normal vascular patterning was restored upon PIN1:GFP expression in the epidermis of *pin1* mutants (Table 1 and Fig. S2 *F–J*). The development of vasculature in the absence of PIN1 activity in internal tissue layers of the leaf may reflect the compensatory action of other PIN protein family members acting redundantly in these tissues. These results indicate that PIN1 activity in the epidermis of the leaf margin underlies both serration and vascular development. To investigate whether these two processes can be uncoupled, we analyzed leaf vasculature in *cuc2* mutants. Although they lack serrations, epidermal PIN1 convergence points, and discrete peaks of auxin activity, *cuc2* leaves mirror wild-type vascular development in secondary vein number, the capacity of veins to branch to the

Table 1. *AtML1::PIN1::GFP* rescues vascular defects in *pin1-7* mutants

Genotype	Average no. of secondary veins in fifth rosette leaf (\pm SE)
Col	9.76 \pm 0.16
<i>pin1-7</i>	12.8 \pm 1.16
<i>AtML1::PIN1::GFP</i>	9.71 \pm 0.30
<i>pin1-7; AtML1::PIN1::GFP</i>	10.38 \pm 0.26

ANOVA *P* value <0.001 for all genotypes differing from *pin1-7*. *n* = 15.

quinternary order, and the ontogeny of *ATHB-8::GUS* vascular marker expression; except that secondary veins do not terminate at the margins of *cuc2* leaves (Table 2 and Fig. S3 *A–F*). Thus, vasculature can, but serrations cannot, form in the absence of epidermal PIN1 convergence points in *cuc2* mutants. These observations indicate considerable modularity in leaf morphogenetic pathways, despite the use of epidermal auxin maxima as a shared patterning cue in wild-type leaves.

The functional importance of interspersed *CUC2* and auxin activity maxima at the leaf margin, together with previous studies (9), suggests the following conceptual model of serration development (Fig. 5*A*). At the heart of the model is a feedback loop between auxin transport by PIN1 (process 1 in Fig. 5*A*) and polar localization of PIN1 by auxin (process 2). Within each cell, PIN1 is polarized toward the neighboring cell with a higher auxin concentration (up-the-gradient polarization model) (10, 11). Operation of this mechanism requires the presence of *CUC2*, which enables the reorientation of PIN1 (process 3). Auxin, in turn, represses *CUC2* expression (process 4), which yields an interspersed pattern of auxin convergence points and *CUC2* activity. In *Arabidopsis* leaves, which grow primarily at the base, this mechanism produces a basipetally progressing sequence of auxin convergence points separated by *CUC2* expression. This pattern controls local rates of margin outgrowth, yielding serra-

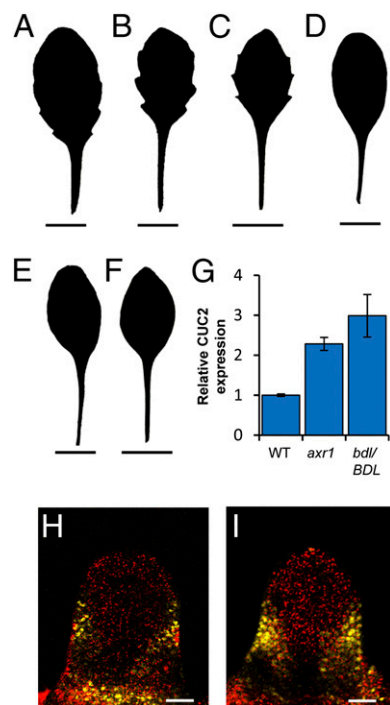


Fig. 3. Auxin regulates leaf margin development via repression of *CUC2*. (*A–F*) Silhouettes of fifth rosette leaf are shown for all genotypes. The auxin signaling mutants *axr1-3* (*B*) and *bdl/BDL* (*C*) have more serrated leaf margins than wild type (*A*). *axr1-3;cuc2-3* (*D*) and *bdl/BDL;cuc2-3* (*E*) double mutants mimic the smooth leaf margins of *cuc2-3* (*F*). (*G*) Quantitative RT-PCR analysis showed that *axr1-3* and *bdl/BDL* plants displayed elevated *CUC2* gene expression compared with wild type. (*H* and *I*) Confocal micrographs showing *CUC2::CUC2::VENUS* expression (yellow) in fifth rosette leaf 125 μ m in length in wild type (*H*) and *axr1-3* (*I*). (Scale bars: *A–F*, 1 cm; *H* and *I*, 25 μ m.) Error bars represent SE of mean from three biological replicates.

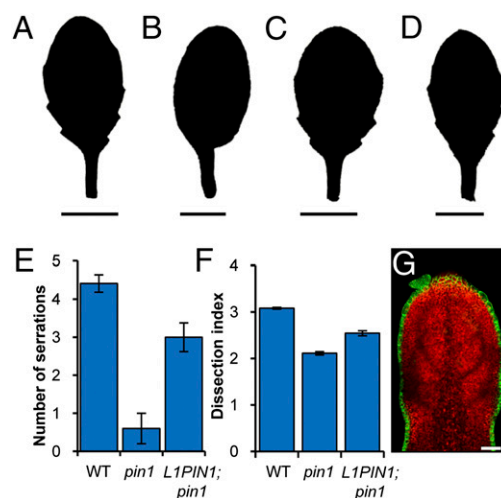


Fig. 4. Epidermal PIN1 activity is sufficient for serration development. (*A–D*) Silhouette of fifth rosette leaf in wild type (*A*), *pin1-7* (*B*), *AtML1::PIN1::GFP* (*C*), and *pin1-7; AtML1::PIN1::GFP* (*D*). (*E*) Quantification of serratation number in fifth rosette leaf of wild type, *pin1-7*, and *pin1-7;AtML1::PIN1::GFP* (*L1PIN1;pin1*). (*F*) Quantification of margin shape using the dissection index (perimeter squared)/(4 π \times area) in fifth rosette leaf of wild type, *pin1-7*, and *L1::PIN1::GFP;pin1-7* (*L1PIN1;pin1*). (*G*) Confocal micrograph of single optical section showing *AtML1::PIN1::GFP* expression (green) in fifth rosette leaf 250 μ m in length. (Scale bars: *A–D*, 1 cm; *G*, 25 μ m.) Error bars represent SE of mean. *n* = 20.

Table 2. Vascular development is similar between *cuc2* mutant and wild-type leaves

Genotype	Average no. of secondary veins in fifth rosette leaf (\pm SE)	Highest minor vein order in fifth rosette leaf
Col	74 \pm 0.15	5
<i>cuc2-3</i>	78 \pm 0.14	5

No difference at 0.1 significance, *t* test *P* value = 0.33. *n* = 15.

tions at sites of high auxin activity and indentations at sites of high CUC2 expression.

Computational Model of Serration Development. We devised a computational model to test whether these molecular-level interactions may plausibly generate observed patterns of gene expression and auxin distribution at the growing leaf margin, as well as the geometric forms of growing leaves. The margin is modeled as a sequential arrangement of cells that propagate through space as the leaf grows (Fig. 5B). Each cell is represented by the positions of its walls in space, concentrations of auxin, PIN1 and CUC2 proteins, and the allocation of PIN1 to the cell membranes abutting adjacent cells. Growth results from a superposition of two processes. The first process coarsely describes the emergence of leaf shape by propagating the margin in the longitudinal and lateral directions independently of auxin and CUC2 concentrations. Consistent with observations of cell division rates by Donnelly et al. (12), we assume that the highest growth rates are near the leaf base. The second process modulates the rates of margin propagation in directions normal to the margin, increasing

them at the sites of high auxin concentration and decreasing them at the sites of high CUC2 expression. Upon reaching a threshold length a cell divides, with the daughter cells inheriting the molecular state of their parent. Details of the model are presented in *SI Materials and Methods* and Fig. S4, with the parameters listed in Tables S2 and S3.

Simulations start with the margin of a leaf primordium modeled as a sequential arrangement of eight cells, with CUC2 expressed in all cells and auxin present in all cells except for the first and last cell in the sequence (Fig. 5C; all simulations are also illustrated in Movies S1, S2, S3, S4, S5, S6, S7, S8, S9, S10, and S11). These two cells act as auxin sinks, sustaining a low concentration of auxin at the boundary between a leaf primordium and the shoot apical meristem throughout the simulation (9). The developmental sequence of a wild-type *Arabidopsis* leaf model is shown in Fig. 5D–H and Movie S1. The earliest developmental stage observed in our data (Fig. 1A) corresponds approximately to frame 20 of the simulations, after which we observed gradual emergence of auxin concentration maxima interleaved with CUC2 expression. These maxima emerge in a basipetal order, where the space for them is created due to high growth rates at the base of the leaf (uniform growth would result in an intercalary order of emergence, Fig. S5I and Movie S8). This process is inherently asymmetric in the proximal–distal direction, producing serrations with larger proximal than distal edges similar to those observed in wild-type *Arabidopsis thaliana* leaves (8). Specifically, a new serration has an adjacent serration in a distal, but not proximal direction. This asymmetry results in a relatively higher number of basal cells supplying auxin to the proximal edge than to the distal edge of the incipient serration, yielding more growth on the proximal side. The growth of the

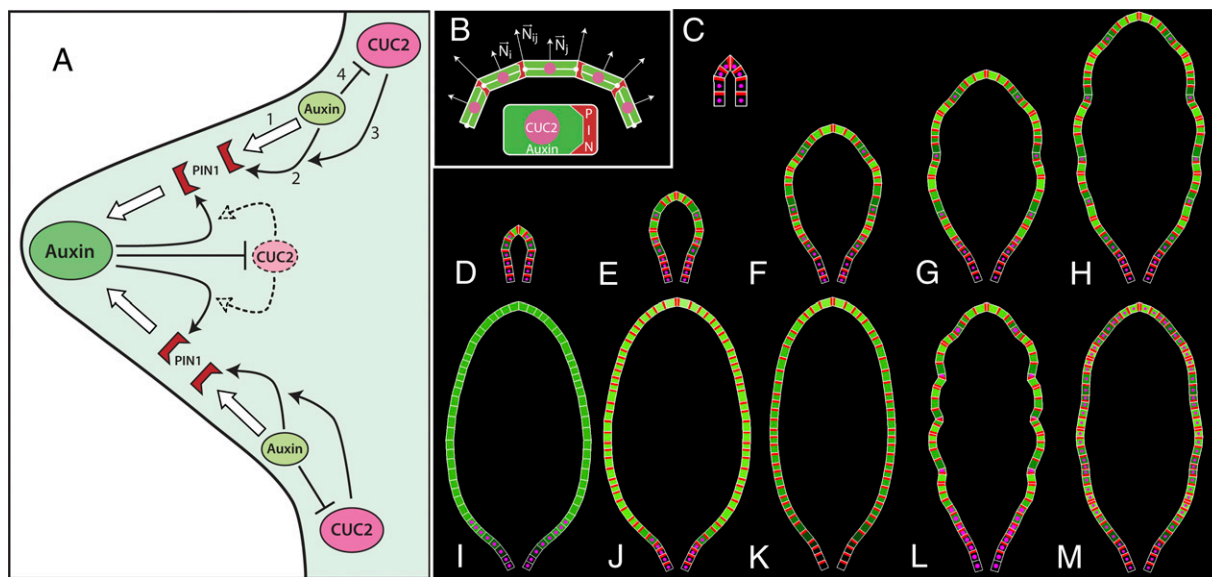


Fig. 5. Conceptual model of interactions between auxin, PIN1, and CUC2 at the leaf margin and leaf simulations. (A) Feedback between auxin transport by PIN1 (process 1) and up-the-gradient polar localization of PIN1 by auxin (process 2) leads to the formation of auxin concentration maxima and minima. Operation of this mechanism requires the presence of CUC2, which enables the reorientation of PINs (process 3). Auxin, in turn, inhibits CUC2 (process 4), which stabilizes the position of auxin maxima. The protrusion and indentations of the serrations are a morphological readout of the sites of high auxin and CUC2 concentrations, respectively. Large and small green ovals, auxin maxima and minima; pink ovals, CUC2 expression; dashed arrows and pale pink oval, CUC2 activity repressed by auxin; red wedges, polarly localized PIN1 proteins. (B) Principle of simulation. A cell is represented as a trapezium, with auxin concentrations shown as a color (black, low concentration; bright green, high concentration), CUC2 concentrations visualized as the radius of a pink circle, and PIN1 concentration at a membrane shown as the width of a red wedge. Leaf development is simulated by iteratively propagating a leaf margin in the normal direction, with auxin locally promoting and CUC2 locally inhibiting the propagation. The propagation is effected by moving cell walls and readjusting cell shapes accordingly. The normal direction N_j at a cell wall is approximated as the average of the normal directions N_j and N_j' of the adjacent cells. (C) Representation of the leaf primordium (frame 1 of the simulation). (D–H) Selected stages of the simulation of wild-type leaf development (frames 127, 284, 651, 990, and 1,350). (I) Simulation of *pin1* mutant produces a leaf without serrations and with auxin concentration gradually decreasing toward the base of the leaf. Related phenotypes characterize a leaf resulting from auxin application (J) and a *cuc2* mutant leaf (K). (L) Increased CUC2 expression produces a leaf with increased indentation. (M) Uniform CUC2 expression produces a leaf with greatly reduced indentation. H–L show frame 1,350 of the simulations.

proximal edge is further enhanced by the assumed gradient of growth rates, decreasing away from the leaf base.

To further validate the model, we simulated the effect of several pharmacological and genetic manipulations and found that they recapitulate our biological observations (Fig. 5 I–M). To simulate *pin1* mutants, we set PIN1 concentration in all cells to 0. Auxin concentration then forms a continuous gradient from the leaf base to the tip (Fig. 5I and Movie S2). The diffuse concentration of auxin irreversibly represses *CUC2* expression outside the leaf base (Eq. S5). In the absence of the pattern of interleaved auxin concentration and *CUC2* expression maxima, no serration is formed (compare with Fig. S3 J–L). Similar model behavior corresponds to simulated N-1-naphthylphthalamic acid (NPA) treatment of the leaf, in which polar auxin transport (parameter T in Eq. S2) is set to 0. Serrations are also absent when exogenous auxin application is simulated by assuming a constant supply of auxin to each cell (parameter Φ_{ext} in Eq. S1). High auxin concentrations repress *CUC2* expression outside the leaf base (Eq. S5), which prevents repolarization of PIN1 (Eq. S4). Consequently, neither *CUC2* expression nor auxin convergence points form (Fig. 5J and Movie S3).

To further investigate the role of *CUC2* in serration formation, we simulated *cuc2* mutant leaves by setting *CUC2* expression to 0 after the PIN1 convergence point at the leaf tip had formed (Fig. 5K and Movie S4), as this convergence point is maintained in *cuc2* leaves (Fig. 2B). The simulated *cuc2* mutant leaves have a smooth margin due to the lack of indentations marked by *CUC2* expression and the lack of protrusions marked by PIN1 convergence points (compare with Fig. S3 M–O). These convergence points do not form as PIN1 fails to repolarize in the absence of *CUC2*. The *cuc2* mutant simulation also captured the dynamic pattern of auxin activity observed during *cuc2* leaf margin development, where a continuous auxin gradient gradually emerges between the minimum at the leaf base and the maximum at the tip. In contrast to these genotypes that lack serrations, leaves with elevated *CUC2* expression have more pronounced serrations, as illustrated by the *mir164a*, *axr1*, and *bdl/BDL* mutants (compare with Fig. S3 P–X). We simulated increased *CUC2* expression by increasing maximum *CUC2* concentration (parameter CUC_{max} in Eq. S5). As anticipated, the resulting model had deeper serrations (Fig. 5L and Movie S5). To investigate the significance of discontinuous *CUC2* expression we simulated uniform *CUC2* expression in each cell. The simulated leaves had reduced depth and number of serrations (Fig. 5M and Movie S6). Models in which a random variation of auxin production (“noise”) was introduced to investigate the robustness of the patterning mechanism further illuminated the role of *CUC2* (Fig. S5 A–H). In the case of uniform *CUC2* expression, auxin maxima moved along the margin. For a moderate amplitude of noise this motion was sporadic, resulting in irregular, asymmetric leaf shapes (Fig. S5 A–C). At higher amplitudes the position of maxima changed frequently, and the lack of sustained maxima resulted in no visible serrations being formed (Fig. S5D). In contrast, the model of a wild-type leaf, which has interspersed *CUC* expression, showed no departure from the deterministic model for moderate noise and approximately correct serrations for high amplitude of noise (Fig. S5 E and F). The feedback between *CUC2* and polar auxin transport is thus essential for the robust formation of serration patterns.

Discussion

Our data indicate that correct PIN1 polarization at the leaf margin requires the presence of *CUC2*. However, computational models suggest that a feedback between PIN polarization and auxin transport alone can produce periodic patterns of PIN convergence points (10, 11), which raises the question of the precise morphogenetic role of *CUC2*. Our model of leaf margin development suggests that the spatially discontinuous expression of *CUC2* has two functions. First, as PIN1 repolarization requires the presence of *CUC2*, localized down-regulation of *CUC2* by auxin stabilizes the position of PIN1 convergence points and auxin maxima on the

margin (Fig. S5 A–H and Movies S7, S9, S10, and S11). Second, *CUC2*-dependent growth repression marks the position of indentations. Thus, *CUC2* is essential to robustly position protrusions and indentations of individual serrations. In the future it will be essential to scrutinize assumptions of the model at the molecular level and understand the molecular events that cause PIN1 proteins to localize against the auxin activity gradient. In this context it will also be important to determine the mechanistic basis through which *CUC2* influences PIN1 polarization and whether *CUC2* also provides PIN1-independent input into cell polarization and tissue patterning. PID family proteins, previously shown to affect PIN1 localization (13), may play a role in these processes.

The positioning of lateral organs at the shoot apex is another process regulated by PIN1 and *CUC* proteins (14), suggesting that *CUC2* may also stabilize PIN1 convergence points during organogenesis. Extending our model to the epidermal layer of the shoot apex may, therefore, improve our understanding of phyllotactic pattern formation by eliminating heuristic assumptions required to properly position and maintain PIN1 convergence points in earlier models (11). The assumption that phyllotaxis can be modeled at the level of the epidermis (10, 11) is further supported by the observation that PIN1 expression, restricted to the epidermis, restores organogenesis and fertility in *pin1* mutants (Fig. S2 K–R).

The proposed model also sheds light on leaf development in other *Arabidopsis* mutants and transgenic plants. For example, leaves with reduced TCP activity have an increased number of serrations (15, 16). According to our model, this increase is a direct consequence of the increased margin length, which creates additional space for serrations to form via *CUC2*, PIN1, and auxin activity. Experimental data support this idea as increased serration of leaves with reduced TCP activity is partially suppressed in a *pin1* or *cuc2* mutant background (Fig. S6 A–F). The repression of *CUC2* by auxin at the leaf margin, shown here, also clarifies the nature of genetic interactions between the *asymmetric leaves1* (*as1*) and *axr1* mutants (4). Specifically, deeply lobed leaf margins form in *as1;axr1* double mutants, where *CUC2* expression is elevated as a consequence of reduced auxin signaling, but not in *as1* mutants alone (Fig. S6 G–I). This enhancement of *as1* reflects *CUC2*-dependent activation of the *KNOX* (*knotted1*-like homeobox) gene *BREVIPEDICELLUS* (*BP*) in the sinus regions of the leaf margin (Fig. S6 J–O). *CUC2*, PIN1, *KNOX*, and TCP proteins are also required for compound leaf development where the margin produces individual leaflets of varied shapes and arrangement (17–24). Extending the framework we propose here to other taxa should thus help to elucidate the molecular mechanisms that underlie the diversity of leaf forms.

In conclusion, serration formation captures two key elements of the broader logic of development. First, morphogenetic information is imparted by discontinuous sequential expression of developmental regulators. Second, temporal periodicity depends on spatial patterning mechanisms that maintain approximately equidistant boundaries of morphogenetically active molecules within developing structures. Such boundaries can be generated by different mechanisms, such as reaction–diffusion, gradient-based positional information, and active auxin transport (which is unique to plants) (25). Our results indicate that growth provides a crucial input to these diverse, independently evolved patterning processes that generate periodic structures and provide a framework for conceptualizing this input.

Materials and Methods

All alleles and transgenic lines (Table S4) were grown on soil under long-day conditions; genetic methods and methods for plasmid construction, analysis of transgenics, treatments using indole-3-acetic acid (IAA) and 2,4-dichlorophenoxyacetic acid (2,4-D), quantitative RT-PCR, leaf clearings, obtaining silhouettes, and quantifying leaf margin shape can be found in *SI Materials and Methods*. Scanning electron microscopy and confocal

microscopy were performed as previously described (26). GUS staining was performed as previously described (7). Models were implemented using the L-system-based modeling software L-studio (<http://algorithmicbotany.org/lstudio>). A detailed model description can be found in [SI Materials and Methods](#). The source code for the models is available on request.

ACKNOWLEDGMENTS. We thank M. Heisler, E. Meyerowitz, J. Traas, D. Wagner, M. Aida, B. Scheres, G. Ingram, D. Weijers, D. Weigel, J. Friml,

S. Hake, N. Ori, U. Grossniklaus, M. Curtis, Nottingham Arabidopsis Stock Centre, and Arabidopsis Biological Resource Center for seed stocks and plasmids. We are grateful to J. Baker for photography, E. Rabbinowitsch for technical assistance, and Yuval Eshed for discussions. This work was supported by a Human Frontier Science Program award (to M.T. and P.P.), Biotechnology and Biological Sciences Research Council Awards BB/G0023905/1, BB/H006974/1, and BB/F012934/1, a Royal Society Wolfson Merit Award, and Gatsby Foundation support (to M.T.), Natural Sciences and Engineering Research Council of Canada awards (to P.P. and A.R.), and a Royal Society University Research Fellowship (to A.H.).

1. Wolfe J-A (1995) Paleoclimatic estimates from Tertiary leaf assemblages. *Annu Rev Earth Planet Sci* 23:119–142.
2. Theophrastus (1916) *Enquiry into Plants, 350–285 BC*, trans Hort A (Harvard Univ Press, Cambridge, MA).
3. Correns C (1909) Inheritance tests with pale (yellow-) green and coloured leafed taxons of *Mirabilis Jalapa*, *Urtica pilulifera* and *Lunaria annua*. *Z Indukt Abstammungs Vererbungsl* 1:291–329.
4. Hay A, Barkoulas M, Tsiantis M (2006) ASYMMETRIC LEAVES1 and auxin activities converge to repress BREVIPEDICELLUS expression and promote leaf development in Arabidopsis. *Development* 133:3955–3961.
5. Nikovics K, et al. (2006) The balance between the MIR164A and CUC2 genes controls leaf margin serration in Arabidopsis. *Plant Cell* 18:2929–2945.
6. Scarpella E, Marcos D, Friml J, Berleth T (2006) Control of leaf vascular patterning by polar auxin transport. *Genes Dev* 20:1015–1027.
7. Sessions A, Weigel D, Yanofsky M-F (1999) The Arabidopsis thaliana MERISTEM LAYER 1 promoter specifies epidermal expression in meristems and young primordia. *Plant J* 20:259–263.
8. Kawamura E, Horiguchi G, Tsukaya H (2010) Mechanisms of leaf tooth formation in Arabidopsis. *Plant J* 62:429–441.
9. Heisler M-G, et al. (2005) Patterns of auxin transport and gene expression during primordium development revealed by live imaging of the Arabidopsis inflorescence meristem. *Curr Biol* 15:1899–1911.
10. Jönsson H, Heisler M-G, Shapiro B-E, Meyerowitz E-M, Mjolsness E (2006) An auxin-driven polarized transport model for phyllotaxis. *Proc Natl Acad Sci USA* 103:1633–1638.
11. Smith R-S, et al. (2006) A plausible model of phyllotaxis. *Proc Natl Acad Sci USA* 103:1301–1306.
12. Donnelly P-M, Bonetta D, Tsukaya H, Dengler R-E, Dengler N-G (1999) Cell cycling and cell enlargement in developing leaves of Arabidopsis. *Dev Biol* 215:407–419.
13. Friml J, et al. (2004) A PINOID-dependent binary switch in apical-basal PIN polar targeting directs auxin efflux. *Science* 306:862–865.
14. Furutani M, et al. (2004) PIN-FORMED1 and PINOID regulate boundary formation and cotyledon development in Arabidopsis embryogenesis. *Development* 131:5021–5030.
15. Efroni I, Blum E, Goldshmidt A, Eshed Y (2008) A protracted and dynamic maturation schedule underlies Arabidopsis leaf development. *Plant Cell* 20:2293–2306.
16. Palatnik J-F, et al. (2003) Control of leaf morphogenesis by microRNAs. *Nature* 425:257–263.
17. Hay A, Tsiantis M (2006) The genetic basis for differences in leaf form between Arabidopsis thaliana and its wild relative Cardamine hirsuta. *Nat Genet* 38:942–947.
18. Barkoulas M, Hay A, Kougioumoutzi E, Tsiantis M (2008) A developmental framework for dissected leaf formation in the Arabidopsis relative Cardamine hirsuta. *Nat Genet* 40:1136–1141.
19. Koenig D, Bayer E, Kang J, Kuhlemeier C, Sinha N (2009) Auxin patterns Solanum lycopersicum leaf morphogenesis. *Development* 136:2997–3006.
20. Shani E, et al. (2009) Stage-specific regulation of Solanum lycopersicum leaf maturation by class 1 KNOTTED1-LIKE HOMEODOMAIN proteins. *Plant Cell* 21:3078–3092.
21. Berger Y, et al. (2009) The NAC-domain transcription factor GOBLET specifies leaflet boundaries in compound tomato leaves. *Development* 136:823–832.
22. Blein T, et al. (2008) A conserved molecular framework for compound leaf development. *Science* 322:1835–1839.
23. Ori N, Eshed Y, Chuck G, Bowman J-L, Hake S (2000) Mechanisms that control knox gene expression in the Arabidopsis shoot. *Development* 127:5523–5532.
24. Hay A, Barkoulas M, Tsiantis M (2004) PINning down the connections: transcription factors and hormones in leaf morphogenesis. *Curr Opin in Plant Biol* 7:575–581.
25. Lewis J (2008) From signals to patterns: Space, time, and mathematics in developmental biology. *Science* 322:399–403.
26. Bowman J-L, Smyth D-R, Meyerowitz E-M (1991) Genetic interactions among floral homeotic genes of Arabidopsis. *Development* 112:1–20.